Dalton Transactions

Accepted Manuscript

ROYAL SOCIETY OF CHEMISTRY

www.rsc.org/dalton

Cite this: DOI: 10.1039/c0xx00000x

www.rsc.org/xxxxxx

ARTICLE TYPE

Syntheses, Crystal Structures, and Optical Properties of Five Metal Complexes Constructed from a V-shaped Thiophene-containing Ligand and Different Dicarboxylate Ligands

Zhi-Qiang Shi,[ab] Zi-Jian Guo[a] and He-Gen Zheng*[a]

Received (in XXX, XXX) Xth XXXXXXXXX 20XX, Accepted Xth XXXXXXXXX 20XX
DOI: 10.1039/b000000x

Five new metal complexes, {[Ni(DIDP)(*m*-bdc)(H_2O)]·5H_2O}$_n$ (**1**), {[Zn(DIDP)(hfipbb)]·2DMA}$_n$ (**2**), {[Zn(DIDP)(4,4'-sdb)]·H_2O}$_n$ (**3**), {[Co(DIDP)(*p*-bdc)]}$_n$ (**4**), and {[Co_2(DIDP)(hfipbb)$_2$]·H_2O}$_n$ (**5**) have been synthesized by reactions of the corresponding metal ions with a V-shaped ligand 2,8-di(1*H*-imidazol-1-yl)dibenzothiophene (DIDP) and different aromatic dicarboxylic acids, namely isophthalic acid (*m*-H_2bdc), terephthalic acid (*p*-H_2bdc), 4,4'-(hexafluoroisopropylidene)bis(benzoic acid) (H_2hfipbb), and 4,4'-sulfonyldicarboxylic acid (4,4'-H_2sdb), respectively. The structures of the complexes were determined by X-ray single-crystal diffraction. Complex **1** is a 1D chain structure containing one-dimensional channel along the *a* direction and further extended via O–H···S hydrogen bonds and C–H···π stacking interactions into a 3D network. Complex **2** exhibits a quasi 2D + 2D → 2D with parallel polycatenation of 2D (4, 4) nets. Complex **3** displays an unusual 2D + 2D→3D parallel polycatenated framework based on a 2D 6^3-hcb network. Complex **4** shows a 2D 4-connected {$4^4.6^2$}-**sql** network containing one-dimensional channel along the *b* direction. The adjacent 2D networks are further extended via C–H···O hydrogen bonds into a 3D supramolecular framework. Complex **5** features a 2-fold interpenetrating 3D framework with 6-connected {$4^{12}.6^3$} **pcu** topology. Furthermore, the thermal stability for **1**−**5**, luminescent properties of **2** and **3** have been studied. Moreover, the solid-state UV-visible spectroscopy experiments show that complexes **1**−**5** are all optical semiconductors with band gaps of 3.06, 3.18, 3.23, 2.98, and 3.17 eV, respectively.

Introduction

Porous metal–organic frameworks (MOFs) are a class of crystalline porous materials[1] and have received tremendous interest in recent years because of their various potential applications in gas storage and separation,[2] catalysis[3], luminescent materials[4], magnetic materials[5], sensors,[6] ion exchange,[7] and so on. Compared to other porous materials, such as zeolites, activated carbon, and covalent–organic frameworks (COFs), the most interesting feature of MOFs is their chemical versatility, due to their chemical composition of metal atoms or metal-containing clusters and organic bridging ligands[8] So the judicious choice of organic bridging ligands is the key point in the construction of desired structural and target functional MOFs.[9] To date, most studies for MOFs focus on adsorption, moleculesensing, and heterogencous catalysis. But the photoelectric properties of MOFs are not well researched.[10] On the other hand, conjugated thiophene compounds have attracted significant attention because of their good electron-transferring abilities and optical absorption properties.[11] However, MOFs constructed from conjugated thiophene-based ligands are rather limited. Therefore, significant research efforts are still need to develop this branch of research. In this text, we designed and synthesized a new V-shaped conjugated thiophene-based organic linker 2,8-di(1*H*-imidazol-1-yl)dibenzothiophene (DIDP) to build a series of metal complexes in the presence of various aromatic dicarboxylic acids. Due to the rotation of the C–N single bonds in the DIDP, two imidazol rings can form different dihedral angles to adjust the coordination orientation of the two nitrogen atoms, thus it may ligates metal centers in different orientations. So, the ligand was proved to be a good candidate for the construction of porous MOFs. Herein, we reported the syntheses and characterizations of five metal complexes: {[Ni(DIDP)(*m*-bdc)(H_2O)]·5H_2O}$_n$ (**1**), {[Zn(DIDP)(hfipbb)]·2DMA}$_n$ (**2**), {[Zn(DIDP)(4,4'-sdb)]·H_2O}$_n$ (**3**), {[Co(DIDP)(*p*-bdc)]}$_n$ (**4**), and {[Co_2(DIDP)(hfipbb)$_2$]·H_2O}$_n$ (**5**), which exhibit abundant architectures from 1D chains to 3D frameworks by the employment of DIDP and four different dicarboxylate ligands, namely isophthalic acid (*m*-H_2bdc), terephthalic acid (*p*-H_2bdc), 4,4'-(hexafluoroisopropylidene)bis(benzoic acid) (H_2hfipbb), 4,4'-sulfonyldicarboxylic acid (4,4'-H_2sdb) (Scheme 1). Their syntheses, crystal structures, UV absorption spectra, thermal and fluorescence properties have been investigated in detail.

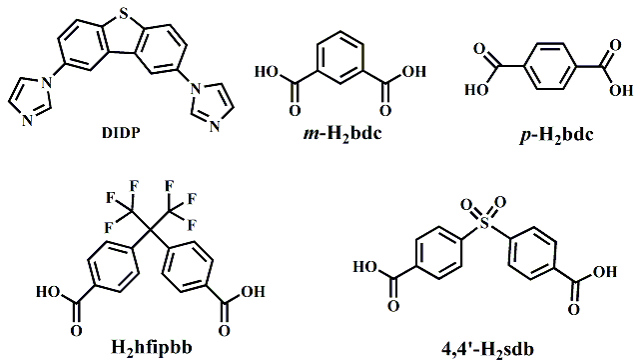

Scheme 1. Structures of N-containing DIDP Ligand and Dicarboxylate Ligands.

Experimental Section

Materials and General Methods

All the chemicals and solvents purchased commercially and used without further purification. DIDP ligand was synthesized by the Ullmann reactions between imidazole and 2,8-dibromodibenzo[*b*,*d*]thiophene (ESI†). C, H, and N analyses were performed on a Perkin Elmer 240C elemental analyzer. IR (KBr pellet) spectra were recorded on a Nicolet Impact 410 spectrometer with KBr pellets in the range of 4000–400 cm^{-1}. Thermogravimetric analyses (TGA) were completed on a Perkin Elmer thermogravimetric analyzer under nitrogen condition at a heating rate of 10 °C·min^{-1}. Powder X-ray diffraction (PXRD) patterns were measured on a Bruker D8 Advance X-ray diffractometer using Mo-Kα radiation (λ = 0.71073 Å) at room temperature. The luminescent spectra for solid samples were conducted with a SHIMAZU VF-320 X-ray fluorescence spectrophotometer at room temperature. Solid UV-visible spectra were obtained on a Shimadzu UV-3600 double monochromator spectrophotometer using $BaSO_4$ as a white standard.

Syntheses of the complexes 1–5

Synthesis of {[Ni(DIDP)(*m*-bdc)(H_2O)]·5H_2O}$_n$ (1)

A mixture of $Ni(NO_3)_2·6H_2O$ (14.5 mg, 0.05 mmol), DIDP (15.8 mg, 0.05 mmol), *m*-H_2bdc (8.3 mg, 0.05 mmol) was dissolved in 6 mL of DMF/H_2O (1:1, v/v). The final mixture was transferred to a Parr Teflon-lined stainless steel vessel (15 mL) under autogenous pressure and heated at 105 °C for 3 days. Green block crystals were collected. Yield: 26% (based on Ni). Anal. calcd for $C_{26}H_{28}N_4NiO_{10}S$: C, 48.24%; H, 4.36%; N, 8.66%. Found: C, 48.21%; H, 4.41%; N, 8.72%. IR(KBr, cm^{-1}): 3417(w), 3135(w), 1664(w), 1604(s), 1544(vs), 1509(s), 1450(m), 1401(s), 1267(m), 1053(w), 845(w), 817(w), 746(m), 724(m), 657(w).

Synthesis of {[Zn(DIDP)(hfipbb)]·2DMA}$_n$ (2)

A mixture of $Zn(NO_3)_2·6H_2O$ (14.9 mg, 0.05 mmol), DIDP (15.8 mg, 0.05 mmol), H_2hfipbb (19.6 mg, 0.05 mmol) was dissolved in 6 mL of DMA/H_2O (1:1, v/v). The final mixture was transferred to a Parr Teflon-lined stainless steel vessel (15 mL) under autogenous pressure and heated at 85 °C for 3 days. Colourless block crystals were collected. Yield: 22% (based on Zn). Anal. calcd for $C_{43}H_{38}F_6N_6O_6SZn$: C, 54.58%; H, 4.05%; N, 8.88%. Found: C, 54.52%; H, 4.09%; N, 8.94%. IR(KBr, cm^{-1}): 3443(w), 3122(s), 1626(vs), 1563(m), 1518(m), 1359(s), 1253(s), 1211(s), 1173(s), 1064(w), 968(w), 842(w), 749(w), 663(w), 567(w).

Synthesis of {[Zn(DIDP)(4,4'-sdb)]·H_2O}$_n$ (3)

A mixture of $Zn(NO_3)_2·6H_2O$ (14.9 mg, 0.05 mmol), DIDP (15.8 mg, 0.05 mmol), 4,4'-H_2sdb (15.3 mg, 0.05 mmol) was dissolved in 6 mL of DMF/H_2O (1:1, v/v). The final mixture was transferred to a Parr Teflon-lined stainless steel vessel (15 mL) under autogenous pressure and heated at 95 °C for 3 days. Colourless block crystals were collected. Colourless block crystals were collected. Yield: 28% (based on Zn). Anal. calcd for $C_{32}H_{22}N_4O_7S_2Zn$: C, 54.59%; H, 3.15%; N, 7.96%. Found: C, 54.53%; H, 3.21%; N, 8.02%. IR(KBr, cm^{-1}): 3457(w), 3130(w), 1622(vs), 1565(m), 1516(m), 1396(s), 1363(s), 1296(w), 1160(m), 1127(w), 1101(w), 1064(w), 745(s), 623(w), 566(w).

Synthesis of {[Co(DIDP)(*p*-bdc)]}$_n$ (4)

A mixture of $Co(NO_3)_2·4H_2O$ (14.6 mg, 0.05 mmol), DIDP (15.8 mg, 0.05 mmol), *p*-H_2bdc (8.3 mg, 0.05 mmol) was dissolved in 6 mL of DMF/H_2O (1:3, v/v). The final mixture was transferred to a Parr Teflon-lined stainless steel vessel (15 mL) under autogenous pressure and heated at 115 °C for 3 days. Purple block crystals were collected. Purple block crystals were collected. Yield: 12% (based on Co). Anal. calcd for $C_{26}H_{16}CoN_4O_4S$: C, 57.89%; H, 2.99%; N, 10.39%. Found: C, 57.84%; H, 3.03%; N, 10.44%. IR(KBr, cm^{-1}): 3419(s), 3088(w), 1594(vs), 1508(s), 1353(vs), 1115(w), 1056(w), 868(w), 820(m), 743(m), 655(w), 521(w).

Synthesis of {[Co_2(DIDP)(hfipbb)$_2$]·H_2O}$_n$ (5)

A mixture of $Co(NO_3)_2·6H_2O$ (29.1 mg, 0.1 mmol), DIDP (15.8 mg, 0.05 mmol), H_2hfipbb (39.2 mg, 0.1 mmol) was dissolved in 6 mL of DMF/H_2O (1:3, v/v). The final mixture was transferred to a Parr Teflon-lined stainless steel vessel (15 mL) under autogenous pressure and heated at 105 °C for 3 days. Dark purple block crystals were collected. Yield: 36% (based on Co). Anal. calcd for $C_{52}H_{30}Co_2F_{12}N_4O_9S$: C, 52.02%; H, 2.52%; N, 4.67%. Found: C, 51.96%; H, 2.57%; N, 4.71%. IR(KBr, cm^{-1}): 3442(m), 3141(w), 1692(m), 126(s), 1566(w), 1511(m), 1406(vs), 1254(s), 1216(w), 1168(s), 1063(w), 967(w), 780(w), 724(m), 479(w).

Single crystal structure determination and refinement

The single-crystal structure data for complexes **1**–**5** were collected on a Bruker Smart Apex II CCD diffractometer using Mo Kα radiation (λ = 0.71073 Å). A semiempirical absorption correction was applied using SADABS program.[12] The structures were solved by direct methods and all non-hydrogen atoms were located from the trial structures and then refined anisotropically on F^2 refined by full-matrix least-squares procedures technique using the SHELXTL[13] crystallographic software package. The organic hydrogen atoms were generated geometrically. The hydrogen atoms of coordinated water molecule in complex **1** were located in the difference Fourier map and refined isotropically. There are some guest solvent molecules in the crystals of **1**, **2**, **3** and **5**, and were chemically featureless to refine using conventional discrete-atom models. Therefore the SQUEEZE program implemented in PLATON[14] was used to remove these electron densities. The details of the crystal parameters are listed in Table 1. The selected bond lengths and angles and hydrogen bond parameters are summarized in Tables S1 and S2 (ESI†). CCDC numbers are 999354-999358 for **1**–**5**, respectively. Topological analyses were performed using the

program package TOPOS.[15]

Description of the crystal structures

{[Ni(DIDP)(*m*-bdc)(H_2O)]·5H_2O}$_n$ (1)

The X-ray crystallographic analysis shows that complex **1** crystallizes in the triclinic space group *P*-1, with an independent Ni(II) cation, one DIDP ligand, one deprotonated *m*-bdc ligand, one coordinated water molecule, and five lattice water molecules squeezed by PLATON software in the asymmetric unit. The Ni(II) cation is coordinated by two nitrogen atoms from two DIDP ligands (Ni–N = 2.058(2)–2.058(2) Å), three oxygen atoms from two *m*-bdc ligands and one oxygen atom from one coordinated water molecule (Ni–O = 2.0202(15)–2.1532(15) Å), and adopts a slightly distorted {NiN_2O_4} octahedral geometry, as shown Figure 1a. The Ni–O/N bond lengths are all normal and comparable to other Ni complexes.[16] The two carboxylate groups of *m*-bdc ligand act as bisdentate-chelating and monodentate modes, respectively, and link the Ni(II) cations to form one infinite 1D linear chain with Ni···Ni distance of 10.163 Å and Ni···Ni···Ni angle of 180.00° (Figure 1b). Two DIDP ligands link two Ni(II) cations to form approximately rhombus [Ni_2(DIDP)$_2$] 26-membered metallamacrocycle (Figure 1c). The supplementary interior angles are 66.8° and 113.2°, respectively. In the metallamacrocycle, the N···Ni···N angle is 177.4°, indicating that the two N atoms and the Ni(II) cation almost in a line. Thus, an interesting 1D chain with a large 1D channel along the *a*-axis is formed (Figure 1d). As depicted in Figure 1e, the adjacent chains are arranged in an AAA type and connected by O–H···S hydrogen bonds to 2D polymeric structure along the *ab* plane. (Table S2, ESI†). Furthermore, the 2D network are held together in a parallel···ABAB··· fashion via C–H···π interactions [H4···*Cg*1^{iii} = 3.21 Å, C4–H4···*Cg*1^{iii} = 146.86°. *Cg*1 is the centroid of the C12–C17 ring; symmetry code: (iii) 1 - *x*, 2 - *y*, 1 - *z*] to generate a 3D extended supramolecular framework (Figure 1f). In addition, intramolecular hydrogen bonds O5-H5B···O2 help to consolidate the crystal structure. PLATON analysis gives the solvent-accessible voids to be 25.1 % (360.4 out of the 1436 Å^3 unit cell volumes) in complex **1**.

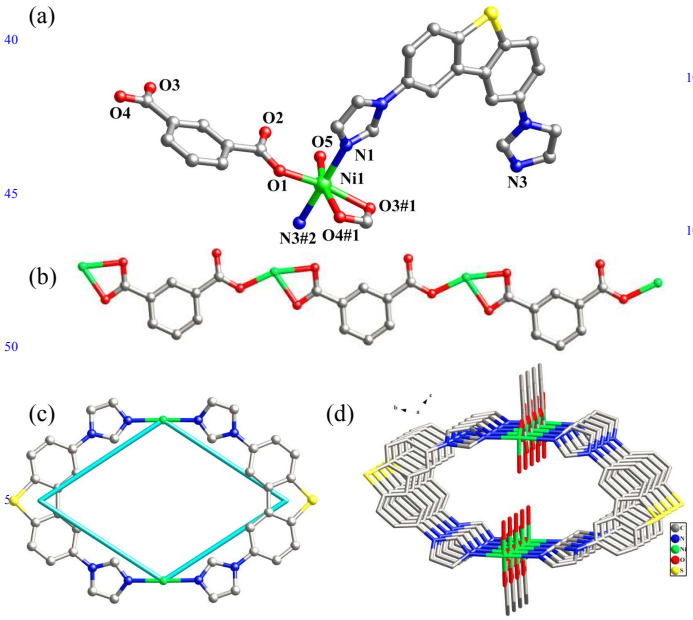

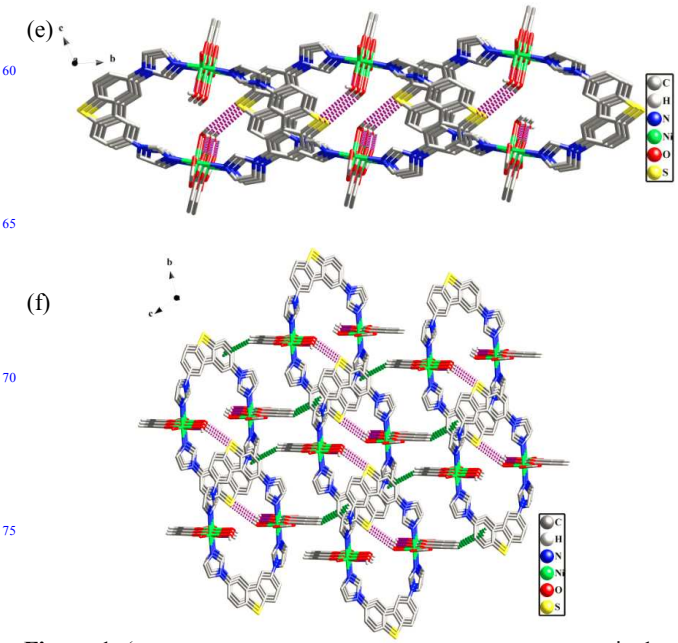

Figure 1. (a) Coordination environment of the Ni(II) cation in **1**. The hydrogen atoms are omitted for clarity. Symmetry codes: #1 = -1+*x*, *y*, *z*; #2 = -*x*, 2-*y*, -*z*. (b) An infinite 1D linear chain formed by the carboxylate groups of hfipbb ligands and the Ni(II) cations. (c) Rhombus [Ni_2(DIDP)$_2$] metallamacrocycle. (d) 1D chain with a large channel of **1**. (e) Perspective of the 2D netwok via the hydrogen bonds (purple dashed line) of **1**. (f) Schematic representation of the 3D framework of **1**. The C–H···π interactions and hydrogen bonds are shown with the green and purple dash lines, respectively.

{[Zn(DIDP)(hfipbb)·2DMA]}$_n$ (2)

The result of X-ray diffraction analysis reveals that complex **2** is a quasi parallel polycatenated 2D + 2D → 2D framework based on an undulated $4^4.6^2$-**sql** square layer. It crystallizes in the triclinic crystal system with space group of *P*-1. The asymmetric unit contains one crystallographically independent Zn(II) cation, one DIDP ligand, one hfipbb ligand, and two free DMA molecules squeezed by PLATON software. As shown in Figure 2a, the Zn(II) cation locates in a {ZnN_2O_2} distorted tetrahedral geometry made up of two N atoms from two symmetrical DIDP ligands and two oxygen atoms from two symmetrical hfipbb ligands. The bond lengths of Zn–O and Zn–N are 1.936(2) Å and 1.990(5)–2.022(7), which are similar to other reported Zn complexes previously.[17] Each hfipbb ligand bridges the adjacent Zn(II) cations to yield one infinite 1D linear chain with Zn···Zn distance of 14.575 Å and Zn···Zn···Zn angle of 180.00° (Figure 2b). The other infinite 1D linear chain with Zn···Zn distance of 14.509 Å and Zn···Zn···Zn angle of 180.00° is also generated by DIDP ligands and the Zn(II) cations (Figure 2b). Then, the two types of 1D chains are linked to generate a 2D network by sharing the Zn(II) cations (Figure 2b). From a topological viewpoint, the Zn(II) cations can be considered as 4-connected nodes. In order to present the real interpenetration of the complex, DIDP and hfipbb ligands can be simplified as V-shaped linkers,[18] so, the whole structure can be simplified to an **sql** network (Figure 2c). It is interesting that the adjacent 2D networks are packed as a quasi parallel 2D + 2D → 2D network, as depicted in

Figure 2d. PLATON analysis gives the solvent-accessible voids to be 32.8% (690.5 out of the 2105.5 Å^3 unit cell volumes) in complex **2**.

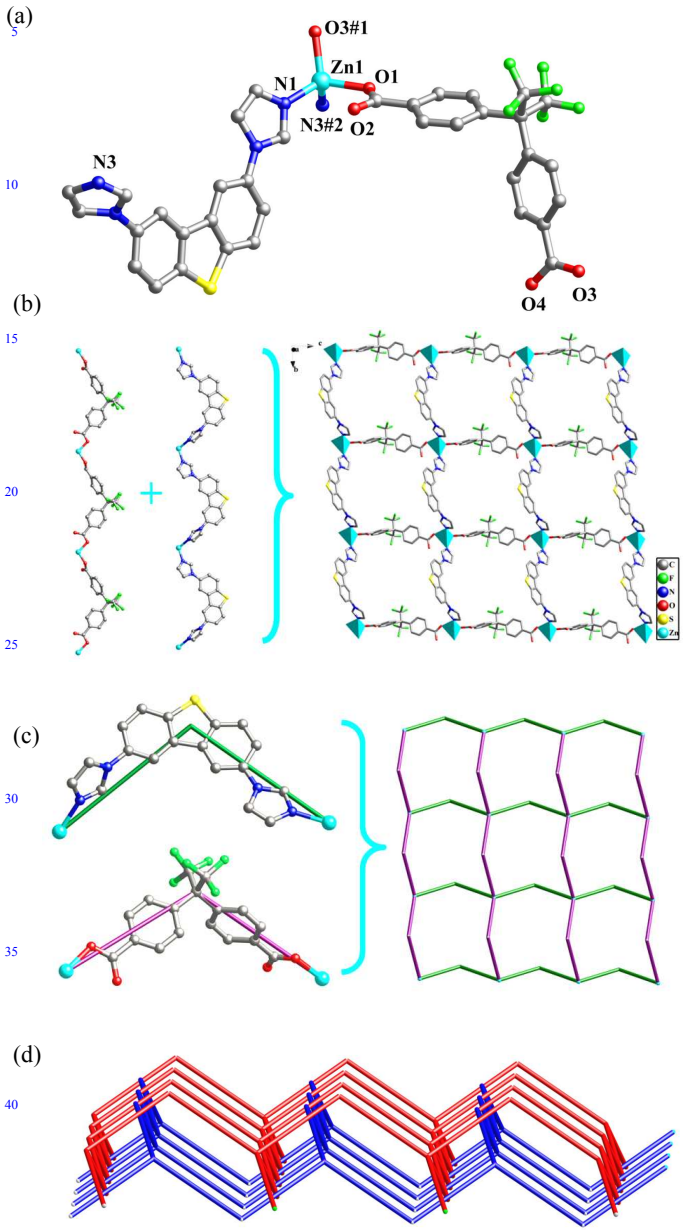

Figure 2. (a) Coordination environment of the Zn(II) cation in **2**. The hydrogen atoms are omitted for clarity. Symmetry codes: #1 = *x*, *y*, 1+*z*; #2 = *x*, -1+*y*, *z*. (b) Left: An infinite 1D liner chain formed by Zn(II) cations and hfipbb ligands. Middle: An infinite 1D liner chain constructed by the DIDP and the Zn(II) cations. Right: 2D network of **2**. (c) Network perspective of the 4-connected **sql** topology in **2**. Turquoise ball, Zn; yellow ball, S; blue ball, N; gray ball, C. (d) Schematic representation of the quasi parallel 2D + 2D → 2D network in **2**.

{[Zn(DIDP)(4,4'-sdb)]·H_2O}$_n$ (3)

X-ray analysis shows that complex **3** is a parallel polycatenated 2D + 2D → 3D framework based on an undulated 6^3-**hcb** single layer. Structural analysis indicates that complex **3** crystallizes in the monoclinic system, *C*2/*c* space group. Similar to the Zn(II) cation in **2**, the Zn(II) cation in **3** exhibits the same coordination geometry, that is, distorted tetrahedral geometry of {ZnN_2O_2} (Figure 3a). The bond distances around the Zn(II) cation are normal. As depicted in Figure 3b, the Zn(II) centers are also linked by the 4,4'-sdb ligands to form one infinite 1D zig-zag chain with Zn···Zn separation of 14.0307 Å and Zn···Zn···Zn angle of 133.54°. Different from the case for complex **1**, there is an approximately rectangular [Zn_2(DIDP)$_2$] 26-membered metallamacrocycle (Figure 3c) formed through the coordination between the DIDP ligands and the Zn(II) cations in complex **3**. The supplementary interior angles are 87.9° and 92.1°, respectively. In the metallamacrocycle, the N···Zn···N angle is 98.9°. Furthermore, a 2D network is formed by the cross-link between the metallamacrocycles and the 1D zig-zag chains (Figure 3d). Topologically, if Zn(II) cations are regarded as 3-connected nodes, and the DIDP and 4,4'-sdb ligands are considered as V-shaped linkers in order to present the real interpenetration of the complex,[18] the framework of complex **3** can be viewed as a 3-connected 6^3-**hcb** net. Noticeably, the 6^3-hcb layers stack with an AAA sequences, and each of these equivalent layers is interdigitated with the adjacent two parallel layers, giving the final 3D supramolecular architecture. So, the most intriguing feature of complex **3** is the 2D + 2D → 3D parallel polycatenation. (Figure 3e).

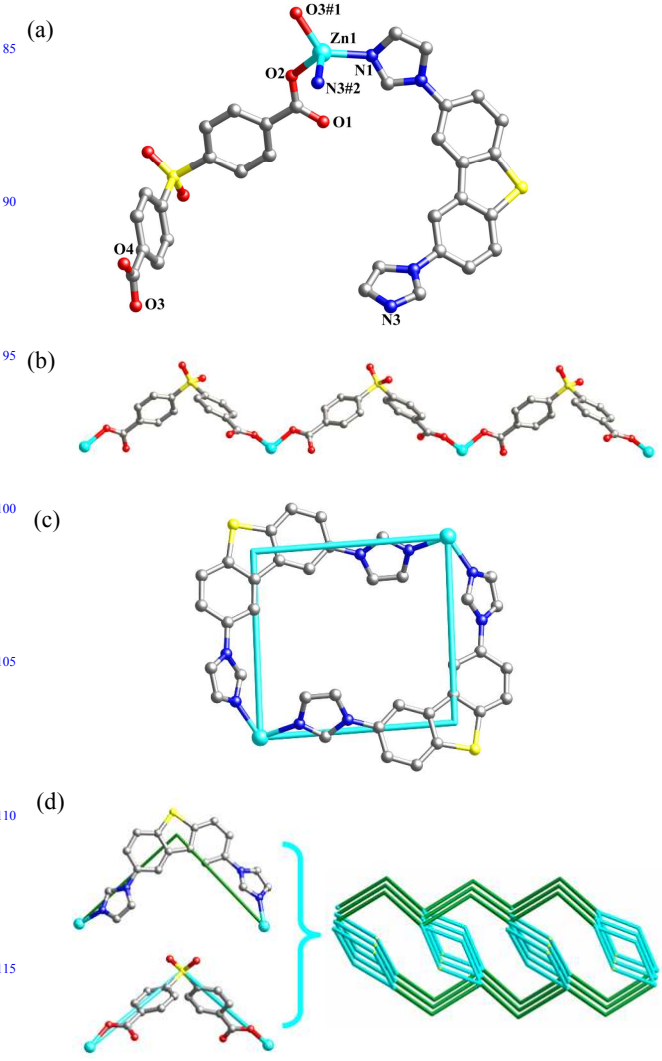

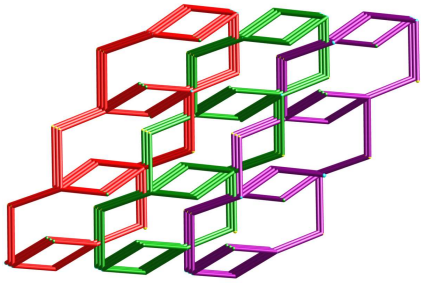

Figure 3. (a) Coordination environment of the Zn(II) cation in **3**. The hydrogen atoms are omitted for clarity. Symmetry codes: #1 = *x*, -*y*, -0.5+*z*; #2 = 0.5-*x*, 0.5-*y*, 1-*z*. (b) An infinite 1D zig-zag chain formed by 4,4'-sdb ligands and the Zn(II) cations. (c) Rectangular $[Zn_2(DIDP)_2]$ metallamacrocycle. (d) Schematic view of 2D netwok of **3**. Turquoise ball, Zn; yellow ball, S; blue ball, N; gray ball, C. (e) Schematic view of 2D + 2D → 3D parallel polycatenation of **3**..

{[Co(DIDP)(*p*-bdc)]}$_n$ (4)

Complex **4** crystallizes in monoclinic space group $P\ 2_1/c$. Its asymmetric unit contains one crystallographically independent Co(II) cation, one DIDP ligand and one deprotonated *p*-bdc ligand. As shown in Figure 4a, the Co(II) center presents a tetrahedral coordination geometry, which is coordinated by two carboxylate oxygen atoms from two *p*-bdc ligands and two nitrogen atoms from two DIDP ligands. It is noteworthy that both *p*-bdc and DIDP ligands link the Co(II) cations to form zig-zag chains with Zn···Zn···Zn angles of 106.544° and 101.727°, respectively (Figure 4b). The combination of the two kinds of 1D chains generates the 2D structure of complex **4** (Figure 4b). The most striking feature of the 2D network is that there exist 1D tubular channels along the *b*-axis (Figure 4c). To better understand the structure of complex **4**, the topological analysis approach was employed. The Co(II) cations can be regarded as 4-connected nodes, and all the organic ligands are considered as linkers, the framework of complex **4** can be simplified to an **sql** net with Schläfli symbol $\{4^4.6^2\}$. Further, these layers stack in an AAA model to construct a 3D supramolecular framework by weak hydrogen bond (C24-H24···O4#3) formed in the adjacent layers (Figure 4d. Table S2, ESI†).

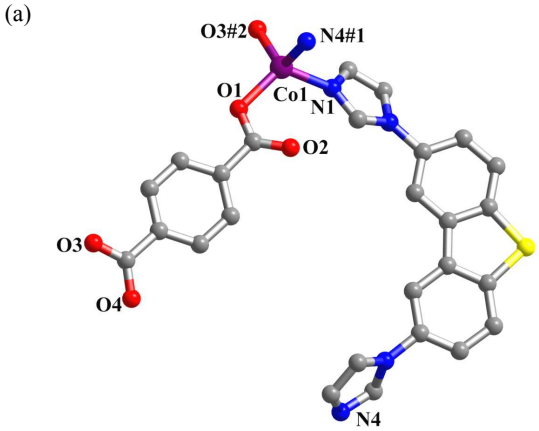

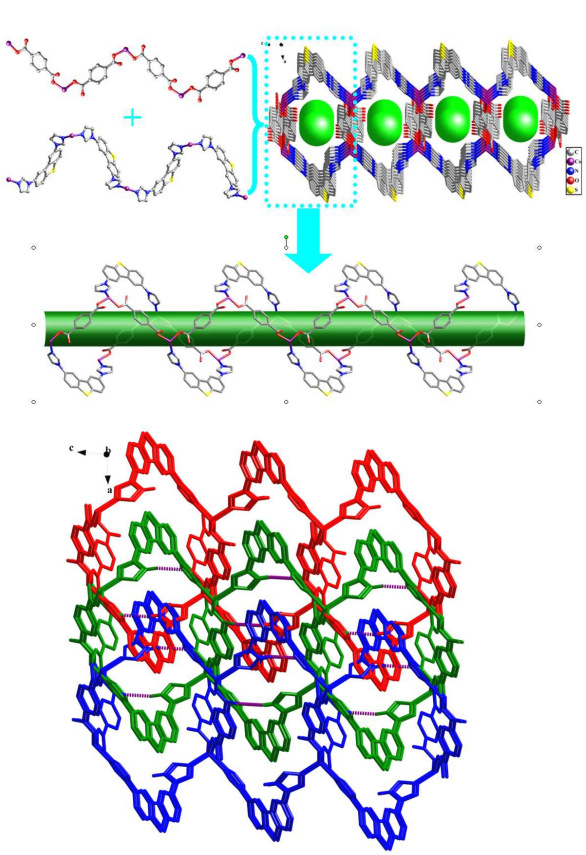

Figure 4. (a) Coordination environment of the Co(II) cation in **4**. The hydrogen atoms are omitted for clarity. Symmetry codes: #1 = *x*, 0.5-*y*, -0.5+*z*; #2 = 3-*x*, 0.5+*y*, 0.5-*z*. (b) Top-left: An infinite 1D zig-zag chain formed by Co(II) cations and *p*-bdc ligands. Bottom-left: An infinite 1D zig-zag chain generated through the DIDP and the Co(II) cations. Right: 2D network of **4**. (c) 1D tubular channels in the 2D network of **4**. (d) View of the 3D supramolecular framework incorporating hydrogen bonds (purple dashed lines).

{$[Co_2(DIDP)(hfipbb)_2]\cdot H_2O$}$_n$ (5)

X-ray single-crystal diffraction analysis reveals that complex **5** is a 3D framework. It crystallizes in the monoclinic crystal system with *P*2/*c* space group. The asymmetric unit of complex **5** is composed of one crystallographically independent Co(II) cation, half of DIDP ligand, one completely deprotonated hfipbb ligand, and one lattice water molecule squeezed by PLATON software. The coordination environment around the Co(II) cation is exhibited in Figure 5a. The Co1 is located in a distorted $\{CoNO_4\}$ square-pyramidal geometry completed by one N atom from one DIDP ligand at the apical position and four O atoms belonging to two symmetrical hfipbb ligands at the basal positions. The Co-N and Co-O bond lengths are all within the normal ranges. Four carboxylate groups from four hfipbb ligands acting as bis-bidentate coordination mode bridge two crystallographically equivalent Co(II) cations to form a "paddlewheel" secondary building unit (SBU), $[Co_2(CO_2)_4]$, with Co···Co distance of 2.8855(3) Å. A 2D layer with a (4, 4) **sql** grid is formed by the constituent square grid, based on the paddle-wheel units and the hfipbb ligands, and has a relatively large diagonal dimension of 14.844 × 23.949 Å^2. On a careful look at the geometry of the 2D

layer, it is observed that left- and right-handed 1D helical chains coexist and array alternately by sharing the paddlewheel SBUs (Figure 5b). As illustrated in Figure 5c, the large rhomboid voids allow the interpenetration between adjacent two layers to occur and form parallel 2D + 2D → 2D network (Figure 5c). The layers are interconnected to form a 3D structure via DIDP ligands with Co···Co distance of 13.758 Å (Figure 5d). Better insight of the complicated 3D architecture can be achieved by topology analysis, so the resulting structure can be reduced to a 6-connected $\{4^{12}.6^3\}$ α-Po **pcu** topology by simplifying the DIDP and 4,4'-sdb as linkers. In order to minimize the large voids in the single net, two equivalent nets adopt 2-fold interpenetration (Figure 5e). However, in spite of interpenetration, the effective free volume of complex **5** is 378.0 $Å^3$ (14.5% of the unit cell volume) as calculated by PLATON.

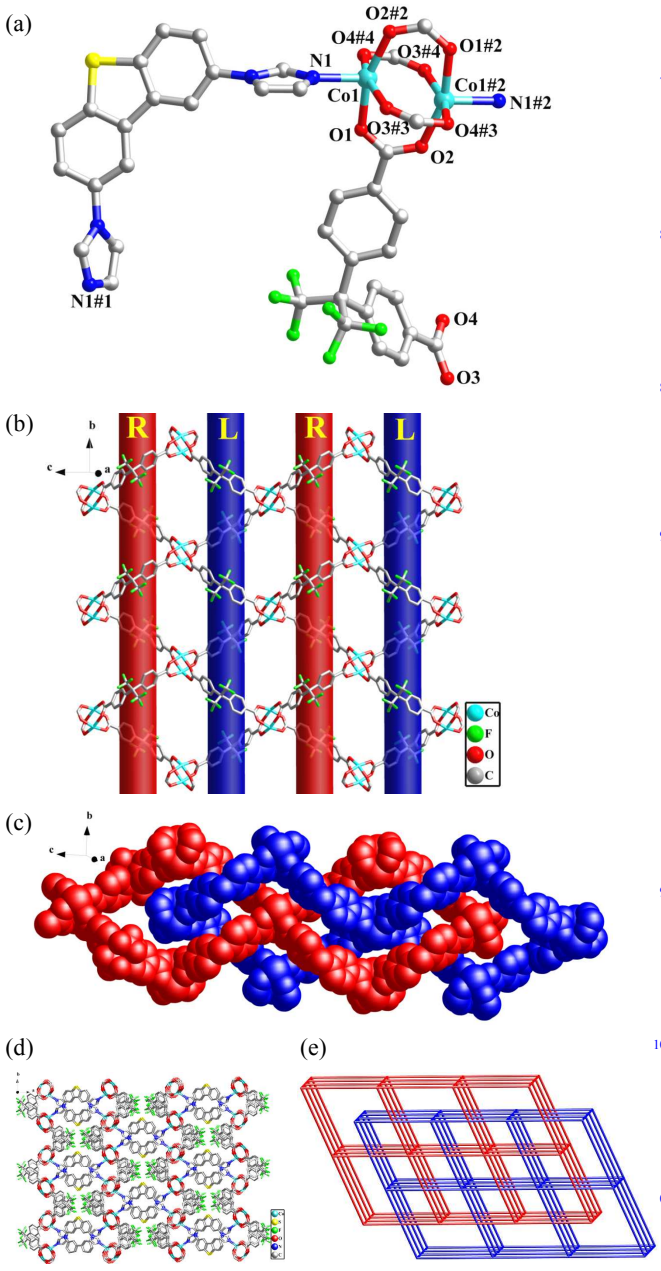

Figure 5. (a) Coordination environment of the Co(II) cations in **5**. The hydrogen atoms are omitted for clarity. Symmetry codes: #1 = 2-*x*, *y*, 1.5-*z*; #2: 1-*x*, 1-*y*, 1-*z*; #3: *x*, -*y*, -0.5+*z*; #4: 1-*x*, 1+*y*, 1.5-*z*. (b) Schematic representation of the left-handed and right-handed helical chains in the 2D network constructed by hfipbb ligands and Co(II) cations in **5**. (c) Space-filling diagram of the 2D → 2D interpenetration in **5**. (d). View of the 3D framework. (e) Schematic view of the 2-fold interpenetrated **pcu** topology of **5**.

Structural Discussion

Five new metal complexes with a V-shaped thiophene-containing ligand and dicarboxylates have been synthesized under similar conditions and described in details. According to the above detailed discussion, we can found that the configuration of imidazole (Im) section of DIDP is key in determining the solid structures of corresponding complexes, because the nitrogen coordination atoms can modulate coordination orientation by rotation of C-N single bonds between Im rings and dibenzothiophene to satisfy the coordination modes. Considering the conformations of Im rings, we defined four important geometric parameters, *α*, *β*, *γ*, and *δ*, which represent the dihedral angles between rings A/B, B/C, C/D, and A/D, respectively (Scheme **2**, ESI†). The details about these dihedral angles are listed in Table **2**.

By comparison, we found that the Im section can tune their conformations to meet the require coordination. Affected by such factors, complexes **1**−**5** show highly diverse structures ranging from 1D chain, quasi parallel 2D + 2D → 2D network, 2D + 2D → 3D parallel polycatenation framework, 2D-**sql** network to 3D 6-connected **pcu** framework.

Table 2. Dihedral Angles between Different Rings in complexes **1-5**

	α	*β*	*γ*	*δ*
1	14.9	2.8	24.9	22.8
2	63.3	1.8	65.4	84.3
3	38.9	3.7	40.8	64.5
4	39.8	4.0	65.6	79.3
5	69.2	2.7	69.2	77.1

PXRD and Thermal Analysis

Powder X-ray diffractions (PXRD) experiments were carried out for **1-5** at room temperature to characterize their purity, as shown in Figures S6- S10 (ESI†). The measured peak positions closely match the simulated peak positions, indicative of pure products.

To characterize the complexes more fully in terms of thermal stability, thermo gravimetric analysis (TGA) were performed on crystalline samples of the title complexes (Figure S11). For complex **1**, the first weight loss of 12.55% (calcd 13.92%) from room temperature to the 124 °C range can be attributed to the loss of lattice water molecules, and the following weight loss from 124 to 184 °C (obsd, 2.34%; calcd, 2.78%) can be ascribed to the removal of coordinated water molecule. After that an additional weight loss corresponding to the decomposition of organic ligands ends at 668 °C with the NiO being the final residue (found 11.86%; calcd. 11.54%). For complex **2**, the preliminary weight loss in the range of 157-245 °C corresponds to the departure of uncoordinated DMA molecule (obsd, 18.5%; calcd, 18.2%), and the solvent-free framework begins to collapse

at 357 °C, leading to the formation of ZnO as the residue (obsd, 8.07%; calcd, 8.60%). For complex **3**, the first weight loss of lattice water molecule is observed in the range of 36-130 °C (obsd: 2.45%; calcd: 2.56%). The decomposition of organic ligands began at 330 °C. For complex **4**, the framework is thermally stable at the temperature of approximately 418 °C, followed by an abrupt weight loss to give the final residual Co_2O_3 (obsd, 16.87%; calcd, 15.37%). For complex **5**, the first weight loss of approximately 1.35% in the range of 76-126 °C is consistent with the loss of free water molecule. Above 356 °C, the whole structure begins to decompose.

Luminescent Properties

The solid-state luminescence spectra of complexes **2** and **3** together with free ligands DIDP, H_2hfipbb and 4,4'-H_2sdb have been investigated at room temperature, as shown in Figure S12 and Table S3 (ESI†). The intense emission peaks appear at 418 nm (λ_{ex} = 295 nm) in **2** and 445 nm (λ_{ex} = 303 nm) in **3**. As for the free ligands, the main emission peaks are located at 435 nm (λ_{ex} = 383 nm) for DIDP, 325 nm (λ_{ex} = 290 nm) for H_2hfipbb, and 344 nm (λ_{ex} = 296 nm) for 4,4'-H_2sdb, which are probably attributed to the $\pi^* \rightarrow$ n or $\pi^* \rightarrow \pi$ transitions. Since the Zn(II) with d^{10} configuration is difficult to be oxidized or reduced, the emissions of **2** and **3** are neither ligand-to-metal charge transfer (LMCT) nor metal-to-ligand charge transfer (MLCT) in nature. In comparison to the free ligands, **2** and **3** exhibit similar emission characters to the free DIDP ligand. So the emission bands of **2** and **3** can probably be attributed to the intraligand fluorescent emission of DIDP ligand.

Optical Energy Gaps

The optical properties of complexes **1**−**5** and free organic ligands were investigated with solid-state UV-vis spectra at room temperature (Figure S13, ESI†). The absorption peaks at 304, 350 nm (DIDP), 292 nm (*m*-H_2bdc), 295 nm (H_2hfipbb), 296 nm (4,4'-H_2sdb), and 313 nm (*p*-H_2bdc) can be ascribed to $\pi \rightarrow \pi^*$ and n $\rightarrow \pi^*$ transitions of the ligands, respectively. For the Ni^{II} and Co^{II}-based complexes, the lower energy band at 620 nm (for complex **1**), 626 nm (for complex **4**), and 613 nm (for complex **5**) are assigned as d-d transitions.[19] The absorption peaks at 342 nm for complex **2** and 343 nm for complex **3** are assigned as ligand-to-metal charge transfer transitions for Zn^{II}-based complexes.[20] In order to investigate the semiconductivity, the diffuse reflectance data were measured and transformed into Kubelka−Munk function to obtain their band gaps (E_g). As shown in Figure S13b, the band gap of DIDP is approximately 3.25 eV, which exhibits the nature of semiconductivity. The E_g values are 3.06 eV for **1**, 3.18 eV for **2**, 3.23 eV for **3**, 2.98 eV for **4**, and 3.17 eV for **5**, respectively, indicating all the complexes are optical semiconductors.

Conclusions

In summary, by using the V-shaped ligand, 2,8-di(1*H*-imidazol-1-yl)dibenzothiophene (DIDP) and a variety of dicarboxylates, we have synthesized five new coordination polymers. Complex **1** features a fascinating 1D channels in the 1D chain structure and further extended into the 3D framework via O–H···S hydrogen bonds and C–H···π stacking interactions. Complex **2** exhibits quasi 2D + 2D → 2D parallel polycatenation. Complex **3** displays an interesting 2D + 2D → 3D framework with parallel polycatenation. Complex **4** is a 2D-**sql** network containing one-dimensional channel and further extended into the 3D framework via C–H···O hydrogen bonds. Complex **5** reveals 2-fold interpenetrating 3D frameworks with $\{4^{12}.6^3\}$ **pcu** topology. The results imply that the combination of V-shaped N-donor ligand with different dicarboxylates can construct MOFs with novel structures and special properties. Furthermore, the UV-vis absorption spectra and optical band gaps of complexes **1**-**5** show that these complexes can be employed as potential semiconductive materials.

Acknowledgements

We gratefully acknowledge the financial support by the Natural Science Foundation of China (21371092; 91022011), and National Basic Research Program of China (2010CB923303).

Notes and references

[a]*State Key Laboratory of Coordination Chemistry, School of Chemistry and Chemical Engineering, Nanjing National Laboratory of Microstructures, Nanjing University, Nanjing 210093, P. R. China, E-mail: zhenghg@nju.edu.cn. Fax: +86-25-83314502.*
[b]*College of Chemistry and Chemical Engineering, Taishan University, Taian 271021, P.R. China*

† X-ray crystallographic data in CIF format (CCDC: 999354-999358 for complexes **1**-**5**), additional figures, FT-IR spectra, TGA curves, UV-vis absorption spectra, patterns of Photochemistry, selected bond distances and hydrogen bond parameters for complexes **1**-**5**. See DOI: 10.1039/b000000x/

1 (*a*) J. S. Li, Y.Y. Chen, Y. J. Tang, S. L. Li, H. Q. Dong, K. Li, M. Han, Y. Q. Lan, J. C. Bao and Z. H. Dai, *J. Mater. Chem. A*, 2014, **2**, 6316; (*b*) H. H. Fei and Seth M. Cohen, *Chem. Commun*., 2014, **50**, 4810; (*c*) H. C. Zhou, J. R. Long and O. M. Yaghi, *Chem. Rev.*, 2012, **112**, 673; (*d*) J. R. Long and O. M. Yaghi, *Chem. Soc. Rev*., 2009, **38**, 1213; (*e*) S. Xiang, Y. He, Z. Zhang, H. Wu, W. Zhou, R. Krishna and B. Chen, *Nat. Commun*., 2012, **3**, 954; (*f*) S. C. Xiang, Z. J. Zhang, C. G. Zhao, K. L. Hong, X. B. Zhao, D. R. Ding, M. H. Xie, C. D. Wu, M. C. Das, R. Gill, K. M. Thomas and B. L. Chen, *Nat. Commun*., 2011, **2**, 204.

2 (*a*) H. T. Kwon and H. K. Jeong, *J. Am. Chem. Soc*., 2013, **135**, 10763; (*b*) H. Wu, Y. S. Chua, V. Krungleviciute, M. Tyagi, P. Chen, T. Yildirim and W. Zhou, *J. Am. Chem. Soc*., 2013, **135**, 10525; (*c*) D. X. Xue, A. J. Cairns, Y. Belmabkhout, L. Wojtas, Y. Liu, M. H. Alkordi and M. Eddaoudi, *J. Am. Chem. Soc*., **2013**, **135**, 7660; (*d*) L. T. Du, Z. Y. Lu, K. Y. Zheng, J. Y. Wang, X. Zheng, Y. Pan, X. Z. You and J. F. Bai, *J. Am. Chem. Soc.*, 2013, **135**, 5622; (*e*) L. Cao, K. Tao, A. Huang, C. Kong and L. Chen, *Chem. Commun*., 2013, **49**, 8513; (*f*) Z. Zhang, Y. Zhao, Q. Gong, Z. Li and J. Li, *Chem. Commun*., 2013, **49**, 653; (*g*) M. P. Suh, H. J. Park, T. K. Prased and D. W. Lim, *Chem. Rev.,* 2012, **112**, 782; (*h*) J. R. Li, J. Sculley and H. C. Zhou, *Chem. Rev*., 2012, **112**, 869; (*i*) K. Sumida, D. L. Rogow, J. A. Mason, T. M. McDonald, E. D. Bloch, Z. R. Herm, T. H. Bae and J. R. Long, *Chem. Rev*., 2012, **112**, 724; (*j*) R. Dawson, D. J. Adams and A. I. Cooper, *Chem. Sci.,* 2011, **2**, 1173; (*k*) D. Zhao,

D. J. Timmons, D. Q. Yuan and H. C. Zhou, *Acc. Chem. Res*., 2011, **44**, 123; (*l*) J. Sculley, D. Q. Yuan and H. C. Zhou, *Energy Environ. Sci.,* 2011, **4**, 2721; (*m*) L. J. Murray, M. Dincâ and J. R. Long, *Chem. Soc. Rev.,* 2009, **38**, 1294.

3 (*a*) M. Aresta, A. Dibenedetto and A. Angelini, *Chem. Rev.,* 2014, **114**, 1709; (*b*) B. Gole, A. K. Bar, A. Mallick, R. Banerjee and P. S. Mukherjee, *Chem. Commun*., 2013, **49**, 7439; (*c*) J. M. Roberts, B. M. Fini, A. A. Sarjeant, O. K. Farha, J. T. Hupp and K. A. Scheidt, *J. Am. Chem. Soc*., 2012, **134**, 3334; (*d*) M. Y. Yoon, R. Srirambalaji and K. Kim, *Chem. Rev.,* 2012, **112**, 1196; (*e*) A. Corma, H. García and F. X. Llabrés i Xamena, *Chem. Rev*., 2010, **110**, 4606; (*f*) Z. Wang, G. Chen and K. Ding, *Chem. Rev*., 2009, **109**, 322; (*g*) J. Lee, O. K. Roberts, J. Farha, K. A. Scheidt, S. T. Nguyen and J. T. Hupp, *Chem. Soc. Rev*., 2009, **38**, 1450; (*h*) L. Ma, C. Abney and W. Lin, *Chem. Soc. Rev*., 2009, **38**, 1248; (*i*) W. Chen, Y. Y. Zhang, L. B. Zhu, J. B. Lan, R. G. Xie and J. S. You, *J. Am. Chem. Soc*., 2007, **129**, 13879; (*j*) K. S. Gavrilenko, S. V. Punin, O. Cador, S. Golhen, L. Ouahab and V. V. Pavlishchuk, *J. Am. Chem. Soc.,* 2005, **127**, 12246; (*k*) C. D. Wu, A. Hu, L. Zhang and W. B. Lin, *J. Am. Chem. Soc*., 2005, **127**, 8940.

4 (*a*) M. Dai, X. R. Su, X. Wang, B. Wu, Z. G. Ren, X. Zhou and J. P. Lang, *Cryst. Growth Des*., 2014, **14**, 240; (*b*) D. X. Li, C. Y. Ni, M. M. Chen, M. Dai, W. H. Zhang, W. Y. Yan, H. X. Qi, Z. G. Ren and J. P. Lang, *CrystEngComm*, 2014, **16**, 2158; (*c*) B. Bhattacharya, R. Dey and D. Ghoshal, *J. Chem. Sci*., 2013, **125**, 661; (*d*) B. A. Blight, R. G. Nicolas, F. KleitzR, Y. Wang and S. Wang, *Inorg. Chem.,* 2013, **52**, 1673; (*e*) Y. J. Cui, F. F. Yue, G. D. Qian and B. L. Chen, *Chem. Rev.,* 2012, **112**, 1124; (*f*) M. D. Allendorf, C. A. Bauer, R. K. Bhakta and R. J. T. Houk, *Chem. Soc. Rev*., 2009, **38**, 1330; (*g*) S. Swavey and R. Swavey, *Coord. Chem. Rev*., 2009, **253**, 2627.

5 (*a*) G. Lorusso, J. W. Sharples, E. Palacios, O. Roubeau, E. K. Brechin, R. Sessoli, A. Rossin, F. Tuna, E. J. L. McInnes, D. Collison and M. Evangelisti, *Adv. Mater.*, 2013, **25**, 4653; (*b*) J. B. Peng, Q. C. Zhang, X. J. Kong, Y. Z. Zheng, Y. P. Ren, L. S. Long, R. B. Huang, L. S. Zheng and Z. P. Zheng, *J. Am. Chem. Soc*., 2012, **134**, 3314; (*c*) P. Dechambenoit and J. R. Long, *Chem. Soc. Rev*., 2011, **40**, 3249; (*d*) D. F. Weng, Z. M. Wang, S. Gao, *Chem. Soc. Rev*., 2011, **40**, 3157; (*e*) M. Nippe, J. F. Wang, E. Bill, H. Hope, N. S. Dalal and J. F. Berry, *J. Am. Chem. Soc*., 2010, **132**, 14261; (*f*) M. Kurmoo, *Chem. Soc. Rev*., 2009, **38**, 1353; (*g*) Y. F. Zeng, X. Hu, F. C. Liu and X. H. Bu, *Chem. Soc. Rev*., 2009, **38**, 469; (*h*) Y. G. Huang, F. L. Jiang and M. C. Hong, *Coord. Chem. Rev*., 2009, **253**, 2814.

6 (*a*) S. S. Nagarkar, B. Joarder, A. K. Chaudhari, S. Mukherjee and S. K. Ghosh, *Angew. Chem., Int. Ed*., 2013, **52**, 2881; (*b*) C. Y. Sun, X. L. Wang, C. Qin, J. L. Jin, Z. M. Su, P. Huang and K. Z. Shao, *Chem.–Eur. J*., 2013, **19**, 3639; (*c*) L. E. Kreno, K. Leong, O. K. Farha, M. Allendorf, R. P. V. Duyne and J. T. Hupp, *Chem. Rev.,* 2012, **112**, 1105; (*d*) Z. Z. Lu, R. Zhang, Y. Z. Li, Z. J. Guo and H. G. Zheng, *J. Am. Chem. Soc*., 2011, **133**, 4172; (*e*) D. Liu, J. P. Lang and B. F. Abrahams, *J. Am. Chem. Soc*., 2011, **133**, 11042; (*f*) J. P. Lang, Q. F. Xu, R. X. Yuan and B. F. Abrahams, *Angew. Chem., Int. Ed*., 2004, **43**, 4741; (*i*) G. J. Halder, C. J. Kepert, B. Moubaraki, K. S. Murray and J. D. Cashion, *Science*, 2002, **298**, 1762.

7 (*a*) B. Manna, A. K. Chaudhari, B. Joarder, A. Karmakar and S. K. Ghosh, *Angew. Chem., Int. Ed*., 2013, **52**, 998; (*b*) C. K. Brozek, A. F. Cozzolino, S. J. Teat, Y. S. Chen and M. Dincă, *Chem. Mater*., 2013, **25**, 2998; (*c*) M. Kim, J. F. Cahill, H. Fei, K. A. Prather and S. M. Cohen, *J. Am. Chem. Soc*., 2012, **134**, 18082; (*d*) Q. Yao, J. Sun, K. Li, J. Su, M. V. Peskov and X. Zou, *Dalton Trans*., 2012, **41**, 3953; (*e*) Z. J. Zhang, W. Shi, Z. Niu, H. H. Li, B. Zhao, P. Cheng, D. Z. Liao and S. P. Yan, *Chem. Commun*., 2011, **47**, 6425.

8 (*a*) B. Bhattacharya, D. Saha, D. K. Maity, R. Dey and D. Ghoshal, DOI: 10.1039/c3ce42441c; (*b*) T. Kajiwara, M. Higuchi, A. Yuasa, H. Higashimura and S. Kitagawa, *Chem. Commun*., 2013, **49**, 10459; (*c*) M. Ranocchiari and J. A. van Bokhoven, *Phys. Chem. Chem. Phys*., 2011, **13**, 6388.

9 S. S. Chen, P. Wang, S. Takamizawa, T. Okamura, M. Chen and W. Y. Sun. *Dalton Trans.*, 2014, **43**, 6012.

10 (*a*) Q. Chen, P. C. Guo, S. P. Zhao, J. L. Liu and X. M. Ren, *CrystEngComm*, 2013, **15**, 1264; (*b*) J. Zhao, X. L. Wang, X. Shi, Q. H. Yang and C. Li, *Inorg. Chem*., 2011, **50**, 3198; (*c*) Q. R. Fang, G. S. Zhu, Z. Jin, M. Xue, X. Wei, D. J. Wang and S. L. Qiu, *Angew. Chem., Int. Ed*., 2006, 45, 6126; (*d*) F. Xamena, A. Corma and H. Garcia, *J. Phys. Chem. C.*, 2007, **111**, 80; (*e*) P. Mahata, G. Madras and S. Natarajan, *J. Phys. Chem. B.*, 2006, **110**, 13759.

11 (*a*) K. Kawabata, M. Takeguchi and H. Goto, *Macromolecules*, 2013, **46**, 2078; (*b*) L. D. Earl, B. O. Patrick and M. O. Wolf, *CrystEngComm*, 2012, **14**, 5801; (*c*) P. M. Beaujjge, S. Ellinger and J. R. Reynolds, *Nature Mat*., 2008, **7**, 795.

12 G. M. Sheldrick, *SADABS Siemens Area Correction Absorption Program*; University of Göttingen: Göttingen, Germany, 1994.

13 Bruker 2000, SMART (Version 5.0), SAINT-plus (Version 6), SHELXTL (Version 6.1), and SADABS (Version 2.03); Bruker AXS Inc.: Madison, WI.

14 Platon Program: A. L. Spek, *Acta Cryst. Sect.* A., 1990, **46**, 194.

15 V. A. Blatov, A. P. Shevchenko and V. N. Serezhkin, *J. Appl. Crystallogr.*, 2000, **33**, 1193.

16 F. L. Hu, Y. Mi, Y. Q. Gu, L. G. Zhu, S. L. Yang, H. Wei and J. P. Lang, *CrystEngComm*, 2013, **15**, 9553.

17 F. L. Hu, W. Wu, P. Liang, Y. Q. Gu, L. G. Zhu, H. Wei and J. P. Lang, *Cryst. Growth Des*., 2013, **13**, 5050.

18 (*a*) X. L. Wang, J. J. Huang, L. L. Liu, G. C. Liu, H. Y. Lin, J. W. Zhang, N. L. Chen and Y. Qu, *CrystEngComm.*, 2013, **15**, 1960; (*b*) X. L. Wang, J. Luan, H. Y. Lin, C. Xu, G. C. Liu, J. W. Zhang and A. X. Tian, *CrystEngComm.*, 2013, **15**, 9995.

19 (*a*) Y. Yang, P. Du, J. Yang, W. Q. Kan and J. F. Ma, *CrystEngComm.*, 2013, **15**, 4357; (*b*) S. Q. Zang, M. M. Dong, Y. J. Fan, H. W. Hou and T. C. W. Mak, *Cryst. Growth Des.*, 2012, **12**, 1239; (*c*) B. K. Tripuramallu, P. Manna, S. N. Reddy and S. K. Das,*Cryst. Growth Des.*, 2012, **12**, 777; (*d*) C. Chen, J. F. Ma, B. Liu, J. Yang and Y. Y. Liu, *Cryst. Growth Des*. 2011, **11**, 4491; (*e*) M. Tonigold, Y. Lu, A. Mavrandonakis, A. Puls, R. Staudt, J. Möllmer, J. Sauer and D. Volkmer, *Chem.–Eur. J.*, 2011, **17**, 8671; (*f*) D. Sarma, K. V. Ramanujachary, S. E. Lofland, T. Magdaleno and S. Natarajan, *Inorg. Chem.*, 2009, **48**, 11660.

20 (*a*) W. W. Xiong, E. U. Athresh, Y. T. Ng, J. F. Ding, T. Wu and Q. C. Zhang, *J. Am. Chem. Soc.*, 2013, **135**, 1256; (*b*) B. Liu,

J. Yang, G. C. Yang and J. F. Ma, *Inorg. Chem*., 2013, **52**, 84; (*c*) J. Guo, J. F. Ma, B. Liu, W. Q. Kan and J. Yang, *Cryst. Growth Des*., 2011, **11**, 3609; (*d*) Y. Xia, P. F. Wu, Y. G. Wei, Y. Wang and H. Y. Guo, *Cryst. Growth Des.*, 2006, **6**, 253.

Table 1. Crystallographic Data and Structure Refinement Details for Complexes **1**-**5**.

Complex	**1**	**2**	**3**	**4**	**5**
Formula	$C_{26}H_{18}N_4NiO_5S$	$C_{35}H_{20}F_6N_4O_4SZn$	$C_{32}H_{20}N_4O_6S_2Zn$	$C_{26}H_{16}CoN_4O_4S$	$C_{52}H_{28}Co_2F_{12}N_4O_8S$
Formula weight	557.21	771.98	686.01	539.42	1214.70
Crystal system	Triclinic	Triclinic	Monoclinic	Monoclinic	Monoclinic
Space group	*P* -1	*P* 1	*C* 2/*c*	*P* 2_1/*c*	*P* 2/*c*
a (Å)	10.1634(8)	11.237(4)	25.388(5)	6.8708(4)	16.3754(8)
b (Å)	11.7309(11)	13.991(5)	10.4704(19)	17.1947(10)	7.4218(4)
c (Å)	13.7734(11)	14.575(5)	25.786(5)	19.5093(11)	23.9485(10
α (deg)	108.547(10)	85.563(8)	90	90	90
β (deg)	97.004(10)	89.011(8)	119.116(5)	96.516(10)	116.683(3)
γ (deg)	107.980(10)	67.178(7)	90	90	90
V (Å^3)	1436.0(2)	2105.5(13)	5988(2)	2290.0(2)	2600.6(2)
Z	2	2	8	4	2
D_{calcd}(g cm^{-3})	1.289	1.218	1.522	1.565	1.551
μ(Mo Ka)(mm-1)	0.787	0.696	1.012	0.884	0.779
F(000)	572	780	2800	1100	1220
Temperature (K)	296(2)	296(2)	296(2)	296(2)	296(2)
θ min-max (deg)	1.61, 25.05	1.58, 25.05	1.81, 25.05	1.58, 25.05	1.39, 25.05
Tot., uniq. data	7912, 5060	11352, 7324	20793, 5312	12784, 4046	18953, 4599
R(int)	0.0165	0.0581	0.0824	0.0252	0.0575
Observed data [$I > 2\sigma(I)$]	3984	3551	4561	3440	4093
N_{ref}, N_{par}	5060, 334	7324, 460	5312, 406	4046, 325	4599, 357
R_1[a],wR_2[b] ($I > 2\sigma(I)$)	0.0355, 0.0926	0.0758, 0.2168	0.0515, 0.1477	0.0306, 0.0910	0.0319, 0.0991
R_1,wR_2 (all data)	0.0476, 0.0971	0.1363, 0.2379	0.0595, 0.1545	0.0387, 0.0955	0.0357, 0.1026
S	1.017	1.024	1.072	1.072	1.003
Min. and max resd dens (e·Å^{-3})	0.362, -0.380	0.582, -0.418	1.027, -0.716	0.291, -0.263	0.344, -0.363

[a] $R_1 = \Sigma||F_0|-|F_c||/\Sigma|F_0|$, [b] $wR_2 = \Sigma[w(F_0^2-F_c^2)^2]/\Sigma[w(F_0^2)^2]^{1/2}$.

5

Graphical Abstract

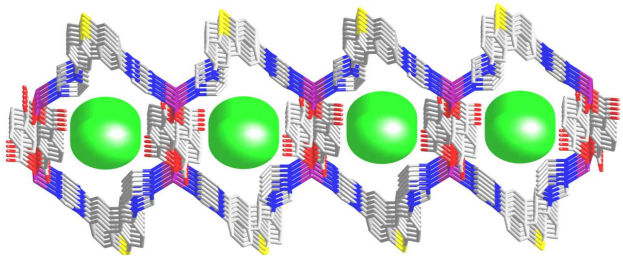

Five new metal complexes constructed from the V-shaped ligand 2,8-di(1*H*-imidazol-1-yl)dibenzothiophene (DIDP) and different aromatic dicarboxylic acids have been synthesized and structurally characterized in detail. All the complexes show optical semiconductive properties.